Particle-shape-, temperature-, and concentration-dependent thermal conductivity and viscosity of nanofluids

Seyed Aliakbar Mirmohammadi,[1] Mohammadreza Behi,[2] Yixiang Gan,[1] and Luming Shen[1,*]

[1]*School of Civil Engineering, The University of Sydney, Sydney, New South Wales 2006, Australia*

[2]*School of Chemical and Biological Engineering, The University of Sydney, Sydney, New South Wales 2006, Australia*

In this study, using the Green-Kubo-method-based molecular dynamics simulations, correlations for predicting the thermophysical properties of nanofluids are developed based on particle shape, fluid temperature, and volume concentration. Silver nanofluids with various nanoparticle shapes including spheres, cubes, cylinders, and rectangular prisms are investigated. The numerical study is conducted within the concentration range 0.14–1.4 vol % and temperature range 280–335 K. The relative thermal conductivity and relative viscosity predicated by the proposed correlations are within a mean deviation of 2% and 5%, respectively, as compared with the experimental results from this study and the available literature. The proposed correlation will be a useful tool for engineers in designing the nanofluids for different applications in industry.

I. INTRODUCTION

Nanofluids, introduced after a pioneering work by Choi and Eastman [1], are engineered colloidal suspensions of nanometer-sized particles in the base fluid. Due to the remarkable alteration to the properties of base fluids after adding nanosized particles, nanofluids have become of great interest in research and industry since their introduction. Metallic nanoparticles such as copper, gold, silver, and carbon nanotubes (CNTs) are common materials dispersed in base fluids like water, ethylene glycol, and so on [2–5].

Nanofluids improve the heat transfer performance and energy efficiency in thermal energy systems. Therefore, they could be used in different industrial applications, such as nanoelectromechanical system technology [6], automobiles [7], solar application [8], and biomedical applications [9]. Thermophysical properties, such as thermal conductivity and viscosity, serve as the most significant characteristics of materials in thermal studies [10]. Hence, accurate prediction and characterization of thermophysical properties play a critical role in the functionality of nanofluids in different applications.

In preparation of nanofluids, researchers have used different highly conductive additives that could be classified into four groups [11]: (i) metallic particles such as Cu, Au, and Ag; (ii) nonmetallic particles such as Al_2O_3, CuO, and SiC; (iii) carbon nanotubes; and (iv) high thermal conductivity nanodroplets. Water is the most investigated liquid in the literature due to its widespread use and ubiquity in our environment. In addition, silver with excellent chemical and physical stability and a wide range of applications is selected as the colloidal suspension to form silver-water nanofluid. However, there are relatively few papers investigating the silver nanofluids. Koca *et al.* [12] evaluated the thermal conductivity, viscosity, and convective thermal performance of the silver-water nanofluid

as a potential working fluid for flat-plate solar collectors. They concluded that silver-water nanofluid is likely capable of being used in flat-plate solar collectors. Based on their study, loading 1 wt. % of silver particles into the water can improve the effectiveness up to 11%. Paul *et al.* investigated the effect of concentration and size of the particle on silver-water nanofluids and a maximum of 21% augmentation was observed in thermal conductivity of nanofluid [13]. Godson *et al.* studied the silver nanofluids under the laminar and turbulent flow conditions and they concluded that silver nanofluids could improve the heat transfer coefficient of the flow by 23.5% and 69% for 0.3 and 0.9 vol % concentrations, respectively [14].

Several experimental and numerical methods have been developed to estimate the thermophysical properties of nanofluids. For example, Xing *et al.* [15] applied a transient hot-wire apparatus for measuring thermal conductivity of CNT-based nanofluids. Another popular experimental method to measure thermal conductivity is called the transient hot-plate method [16]. This method offers some advantages such as fast and easy measurement and flexible sample size [17]. In both of the aforementioned methods, the sensor and probe act as both the heating source and thermometer and Fourier's law for conduction heat transfer is utilized to measure the thermal conductivity of materials [16]. Many attempts have been made to measure the viscosity of nanofluids as well. Over the years, the conventional viscometers such as a falling ball, capillary viscometer, rotating viscometer, etc., have been replaced by faster, more reliable, and more easily operated devices such as coaxial cylindrical rheometers [18].

However, in many cases experimental measurement can only provide limited insight into the mechanism of thermophysical properties changing as a function of certain parameters. As a result, theoretical analysis, mathematical models, and related computer simulations are carried out in the hope of understanding the properties of assemblies of molecules and the microscopic interactions between them. A variety

———————
*Corresponding author: luming.shen@sydney.edu.au

of modeling techniques have been developed for calculating the thermophysical properties over the years [19–21]. Among them, molecular dynamics (MD) simulation can provide detailed atomic-level information and has been widely employed in many numerical studies on the thermophysical properties of fluids [22–24].

Molecular dynamics simulations for calculating thermophysical properties of liquids could be categorized into two types, namely, nonequilibrium molecular dynamics (NEMD) and equilibrium molecular dynamics (EMD) [25,26]. In EMD simulation, the Green-Kubo method, introduced by Green [27] and Kubo [28], has been well established and widely used for calculating thermophysical properties of liquids. This method is based on the Green-Kubo formulation where thermal conductivity and viscosity can be calculated by integrating over time the ensemble average of the autocorrelation of the external field [29]. The authors of the present paper have noticed that the current method of data collection in MD simulation is questionable. Therefore, we have developed a data analysis procedure for calculating the thermal conductivity and viscosity of liquids using MD. Based on our approach, more reliable thermophysical properties of liquids with controllable standard deviation can be obtained using MD simulations [30]. In contrast, in the NEMD simulations, an external field such as shear force or heat flux needs to be applied to create a shear flow or temperature gradient, respectively. Then the desired properties are monitored and calculated [31].

In contrast, the literature suggests that several parameters could have an impact on the thermal conductivity and viscosity of nanofluids, and based on these parameters many correlations have been developed for these effective properties (see, e.g., [32]). For instance, temperature, concentration, particle size, particle shape, and interfacial layers are recognized as parameters affecting the thermal conductivity and viscosity of nanofluids. Das *et al.* investigated water-based nanofluids including CuO and Al_2O_3 in the range 20 °C–50 °C and showed that the thermal conductivity of the nanofluid is temperature dependent [33]. Nguyen *et al.* [34] measured the viscosity of CuO and Al_2O_3 water-based nanofluids with different particle diameters. The results showed the dependence of the viscosity on the temperature and particle size. They also proposed two models to predict viscosity as a function of temperature [34]. Eastman *et al.* performed research on ethylene-glycol-based nanofluids containing copper nanoparticles and showed the relationship between the concentration and thermal conductivity of nanofluids [35]. Moreover, the viscosity has been found to strongly depend on the particle volume fraction as the increase in concentration of nanoparticles raises the viscosity of the nanofluids [36].

As compared with the other parameters, the effect of particle shape is less frequently studied and available literature on this topic is mainly focused on experimental studies. For example, Timofeeva *et al.* [37] measured the thermal conductivity and viscosity of various shapes of alumina nanoparticles in a fluid consisting of equal volumes of ethylene glycol and water. They pointed out that the interaction between base fluids and nanoparticles in determining the enhancements of thermophysical properties is complex [37]. In terms of viscosity models for nanofluids, they focused on the effect of

temperature and concentration. The main reason why other parameters, such as particle shape, structure, and particle size, are less frequently considered is that these models have been mainly obtained by experimental data fittings so far. Thus, a systematically parametric study is restricted by the number of different sample types and it is hard to effectively include all the above-mentioned particle-related parameters in the models [38].

In addition, identification of the relevant particle shape factor seems to be a challenging task. Hamilton and Crosser [39] are known as the pioneers who identified the shape factor for predicting the relative thermal conductivity of the mixtures with different particle shapes. Their empirical shape factor n is defined as $n = 3/\varphi$, where φ is the sphericity and is defined as a ratio of the surface area of the sphere with equal volume to the surface area of the real particle [39]. However, the predictions from the proposed Hamilton-Crosse (HC) model do not agree well with many nanofluid experimental studies because it has been basically developed for micron- or millimeter-sized particles [12]. In recent years, several models have been developed for predicting the relative thermal conductivity of nanorods [40] and CNTs [41]. However, there is no model that could effectively predict the particle shape dependence of the thermal conductivity and viscosity of nanofluids. Therefore, it is worth covering this gap in the literature with further in-depth studies using molecular dynamics simulations.

Since existing correlations have failed to accurately predict the phenomenal changes in thermophysical properties of nanofluids when different particle shapes are used, an effort will be made to derive more accurate correlations. In this study, three parameters, particle shape, temperature, and volume concentration, will be considered to investigate their effect on the viscosity and thermal conductivity of silver nanofluid using EMD simulation. First, the approach developed by Mirmohammadi *et al.* [30] will be used to ensure the reliability of the results obtained from the EMD simulations. Then the model will be validated by our experiment, which will be conducted for silver nanofluids with spherical nanoparticles at different temperatures and volume loadings, as well as other experimental data available in the literature.

II. METHODOLOGY

In this section, first, the method of calculating thermal conductivity and viscosity by employing the Green-Kubo-method-based EMD simulation will be described and then the instruments used to experimentally measure the thermal conductivity and viscosity of silver particle nanofluid will be briefly explained. Finally, the approach to identifying the relevant shape factor will be described.

In this paper, first, several EMD simulation sets, using our sampling and data collection approach reported in [30], will be completed to calculate thermal conductivity and viscosity of silver nanofluid. In these EMD simulations, the effect of volume concentration, temperature, and particle shape will be investigated. Second, based on these EMD simulation results obtained by the parametric study, two correlations will be obtained through dimensional analysis. Finally, the correlations constructed will be benchmarked against data available in the literature as well as our experimental data.

A. Molecular dynamics simulation

1. Thermal conductivity calculation

When a liquid system is in equilibrium, it has a constant average temperature and an average heat flux of zero over a finite time period. However, the temperature fluctuates instantaneously, and as a result, a finite heat flux exists at each instant of time [42]. This phenomenon is the base of the Green-Kubo (GK) method to calculate thermal conductivity and viscosity in EMD simulations.

In macroscopic scale study, thermal conductivity k is a coefficient that relates the macroscopic heat current vector $\boldsymbol{J}$ to the temperature T gradient in the form of Fourier's law

$$\vec{j} = -k\overrightarrow{\Delta T}. \tag{1}$$

However, in a microscopic-scale study, in order to calculate the thermal conductivity k using EMD simulation, the GK method relates the lattice thermal conductivity of the system to the integral of the average of the time correlation function of the heat current by the relation [28,43]

$$k = \frac{1}{3Vk_BT^2}\int_0^\infty \langle\vec{j}(t)\vec{j}(0)\rangle dt, \tag{2}$$

where $\vec{j}(t)$ and $\vec{j}(0)$ are the instantaneous microscopic heat current vectors at time t and time zero, respectively. The angular brackets denote an autocorrelation function, V is the volume of the liquid, and k_B is Boltzmann's constant. The integral calculates the heat autocorrelation function (HACF) and it uses the time needed for the HACF to decay to zero. More details about the Green-Kubo method can be found in [44].

Heat flux is calculated using three different fluctuation modes carried by kinematic energy, potential energy, and energy from the collision of atoms. The expression for the heat flux is

$$
\begin{aligned}
\vec{j} = {} & \sum_{a=1}^{2}\sum_{i=1}^{N_a}\frac{1}{2}(m_a)_i v_{ia}^2 \cdot \vec{v}_{ia} \\
& + \frac{1}{2}\sum_{a=1}^{2}\sum_{b=1}^{2}\sum_{i=1}^{N_a}\sum_{j=1}^{N_b}\left[u(r_{a_i b_j}) - r_{a_i b_j}\frac{\partial u(r_{a_i b_j})}{\partial r_{a_i b_j}}\right]\cdot\vec{v}_{ia} \\
& - \sum_{a=1}^{2}h_a\sum_{i=1}^{N_a}\vec{v}_{ia},
\end{aligned}
\tag{3}
$$

where i and j represent atoms i and j, v is the velocity, r is the distance, u is the interatomic potential energy, m is the mass, and h is the enthalpy. The subscripts a and b denote two different types of particles, while i and j are the numbers of particles; N_a and N_b are the numbers of particles of types a and b. It can be seen that the partial enthalpy term is deducted from the overall heat flux as suggested in [45,46]. It should be noted that, due to the accurate and effective statistical data processing approach [30], the simulation results of the heterogeneous system of nanofluid are in very good agreement with the available literature. Thus, Eq. (3), which was developed for homogeneous systems, can be used in our study.
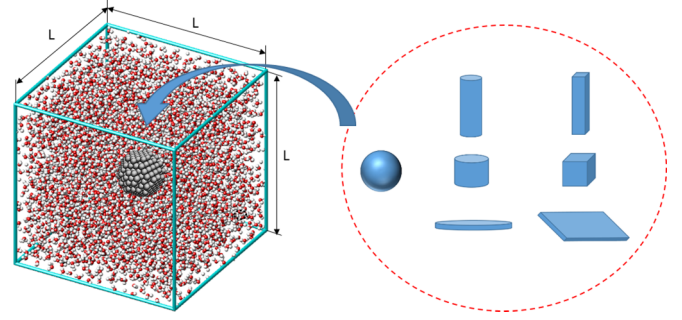

FIG. 1. Silver particles with different shape to be inserted in the MD simulation box filled with water.

2. Viscosity calculation

To calculate the viscosity, the same methodology as described in the preceding section is used. However, the heat autocorrelation function is replaced by the stress (pressure) autocorrelation function (SACF) in the GK equation. The time needed for the SACF to decay to zero is then used through the GK relation to predict the viscosity [47] as

$$\eta = \frac{V}{k_B T}\int_0^t \langle P_{XY}(0)P_{XY}(t)\rangle dt, \tag{4}$$
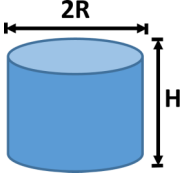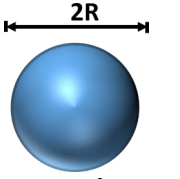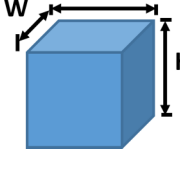
where η is the shear viscosity, V is the volume of the system, and P_{XY} refers to an independent component of the shear stress in the XY direction. However, for an isotropic homogeneous fluid in the absence of external fields, the symmetry of the cubic simulation box implies that the three directions X, Y, and Z are equivalent in this equation. As a result, all three independent off-diagonal elements of the stress tensor are used in the calculation [48].

3. MD simulation model

In this paper, the MD simulation system consists of water liquid as the base fluid and silver nanoparticle. Figure 1 shows the cubic simulation box with periodic boundary conditions in all three directions and different shapes of the silver nanoparticle simulated in this study. Three major shapes are considered, a sphere, cylinder, and rectangular prism, with different aspect ratios that are shown in the figure. Table I presents the dimension and shape of the silver particles used to simulate the thermal conductivity and viscosity of silver nanofluid.

To model the water molecule, the extended simple-point charge (SPC/E) force field is used, where $q_0 = -0.874e$ and $q_H = 0.437e$, with e being the electron charge unit. In addition, for the SPC/E water model, the O-H bond length is 0.1 nm and the H-O-H angle is 109.47°. The H-H and H-O interactions between two different water molecules are ignored due to the small mass of the H atom [49]. The widely accepted 12/6 Lennard-Jones potential, together with a Coulombic term, however, is used to model the interatomic interactions between oxygen atoms of different water molecules, as given

TABLE I. Shape and dimensions of each nanoparticle simulated.

	W (Å)	R or L (Å)	H (Å)	Elongation	Area-based sphericity	Volume-based sphericity	S/V (Å^{-1})
		27	4.5	6	0.76	0.50	0.52
		28	5.5	5.1	0.77	0.53	0.44
		14	15.5	1.11	1.85	1.70	0.27
		19.8	8	2.48	0.84	0.67	0.35
		11.8	22.5	1.91	1.26	1.18	0.26
		7.15	67	9.37	0.49	0.41	0.31
		8	48	6	0.62	0.55	0.29
		13.5		1	1	1	0.22
		20.08		1	1	1	0.15
		21.47		1	1	1	0.14
		23		1	1	1	0.13
		30		1	1	1	0.10
		60		1	1	1	0.05
	21.3	21.3	21.3	1	0.98	0.88	0.28
	12.9	13	58	4.50	0.55	0.45	0.34
	6.5	26	60	9.23	0.56	0.41	0.42
	50	50.07	4.1	12.21	0.86	0.54	0.57
	40	41	6	6.83	0.89	0.64	0.43
	40	40	7	5.71	0.91	0.68	0.39
	41.5	41.5	5.3	7.83	0.89	0.62	0.47

by

$$u_{ab} = \sum_i^{N_a} \sum_j^{N_b} \frac{K_C q_{a_i} q_{b_j}}{r_{a_i b_j}}$$
$$+ \sum_i^{N_a} \sum_j^{N_b} 4\varepsilon_{a_i b_j} \left[\left(\frac{\sigma_{a_i b_j}}{r_{a_i b_j}} \right)^{12} - \left(\frac{\sigma_{a_i b_j}}{r_{a_i b_j}} \right)^6 \right], \quad (5)$$

where subscripts i and j denote atoms i and j in one individual molecule in both terms of Eq. (5), K_C denotes an electrostatic constant, and a and b denote two different molecules.

Two common potential models for metals, namely, the embedded-atom method [50] and the Morse potential [51], are investigated for the silver-silver interaction. Our simulation results for relative thermal conductivity and relative viscosity show a better match to the experimental data using the Morse potential. Therefore, the Morse potential is used to describe the interaction between silver atoms in this paper. The potential energy of two silver atoms i and j with a distance of r can be expressed as

$$u_{\mathrm{Morse}} = D_0 [e^{-2\alpha(r-r_0)} - 2e^{-\alpha(r-r_0)}]. \quad (6)$$

The value of D_0 is adjusted to match the experimental value for the adsorption energy, while r_0 is chosen to give the experimental equilibrium distance of the silver atoms. The Morse potential used in the MD code employs parameters obtained by Girifalco and Weizer [51] using experimental values for the energy of vaporization, the lattice constant, and the compressibility: $D_0 = 0.3323$ eV, $r_0 = 3.155$ Å, and $\alpha = 1.3690$ Å^{-1}, respectively.

The interaction between silver and water is also modeled with the Lennard-Jones potential in Eq. (5) and the parameters used for silver-water interactions are obtained from Ref. [52].

The interactions parameters between silver and hydrogen and between silver and oxygen are $\sigma_{\mathrm{H\text{-}Ag}} = 2.52$ Å, $\sigma_{\mathrm{O\text{-}Ag}} = 2.676$ Å, and $\varepsilon_{\mathrm{H\text{-}Ag}} = \varepsilon_{\mathrm{O\text{-}Ag}} = 0.005\,617$ eV.

In this study, LAMMPS software [53] is used to execute the proposed EMD simulation. A particle-particle–particle-mesh solver is used for the long-range Coulombic interactions [54]. In our EMD simulation, the system is first relaxed under an *NVT* or canonical ensemble, where the volume is kept constant to ensure a given density at a certain temperature by using a Nosé-Hoover thermostat [55] for 20 ps. The system is then switched to an *NPT* or constant pressure and temperature ensemble using a Nosé-Hoover barostat for 25 ps. Finally, an *NVE* ensemble is used to maintain the constant energy and volume of the system for 60 ps before data collection starts. It should be noted that cases with longer running time for each stage are also tested and no noticeable changes are observed.

Considering the fact that previous methods of data collection in MD simulations are questionable, a different data processing method, which has been well documented in [30], will be used to calculate the thermal conductivity and viscosity of liquids in this study. In this data processing method, first, a simulation time after which the standard deviation of the value is below a given limit is determined. Then the average value of the simulated data points collected between this time and the end of the simulation will be obtained. Finally, multiple independent MD simulations with different initial atomic velocity distribution will be performed and their average result will be reported as the property (thermal conductivity or viscosity). Based on this method, more reliable thermophysical properties of liquids with controllable standard deviation can be obtained using MD simulations. For the purpose of simplicity, the details of this method are not repeated here and readers are referred to [30] for more details.

B. Experimental investigation

1. Preparation of nanofluids

Silver nanoparticles were purchased from Research Nanomaterials Ltd., USA. The water used in all experiments was purified with a Milli-Q system. We used two mechanical treatments based on a two-step method to make the complex fluids. The nanofluids were prepared by uniformly dispersing spherical solid nanoparticles with a size range of 50–80 nm (65 nm on average) and volume fraction of 0.005–0.6 vol % in base fluids using a high-pressure homogenizer for an hour (four cycles) and tip sonication for 30 min to ensure appropriate dispersion of the nanoparticles. The volume fraction of the nanofluids was calculated based on the weight and density of the base fluids (ultrapure water, $\rho = 0.998\,21$ g/cm^3) and nanoparticles (silver, $\rho = 10.490\,00$ g/cm^3) at ambient temperature. It should be noted that the effect of temperature on the variation of the volume fraction is considered to be negligible throughout the paper.

All measurements were performed for fresh samples and each experimental run took less than 20 min, including the time required for the temperature stability of the sample holder in the thermal bath. Before each measurement, we ran 20-min bath sonication to ensure minimizing the agglomeration. The prepared nanofluids showed reasonable stability in the period of measurements. Then the sample was ready for measurement. It should be noted that particle size was measured before and after each test (both viscosity and thermal conductivity measurements) to ensure that the quality of the suspension was satisfactory.

2. Experimental apparatus

The Hot Disk Thermal Constants Analyser (Hot Disk AB, Gothenburg, Sweden and ThermTest Inc.) employs the transient plane source technique which can measure the in-plane and through-plane thermal conductivity of the isotropic or anisotropic materials in the same test [16]. In this study, a Hot Disk 500 S (HDS) and standard isotropic method were used. The HDS is capable of measuring thermal conductivity from 0.03 to 100 W/(m K). The sensor employed in this test method was calibrated and optimized with a comprehensive experimental data set. In particular, the sensor was tested for different base liquids (ultrapure water, water-ethylene glycol mixture, and pure ethylene glycol) in the temperature range of 20 °C–50 °C. More than 100 sample data points at the optimized setting were collected to ensure the precision of the measurements.

The viscosity of the nanofluid was measured by an Anton Paar MCR 502 rheometer (Anton Paar, Graz, Austria) using a concentric cylinder measuring unit C-PTD200 with a gap of 0.5 mm and a Peltier temperature-controlled measuring system. This viscometer operates based on the drive of an immersed spindle through a calibrated spring. A known force-to-torque proportion to the viscous drag of the fluid against the spindle is measured by spring deflection. The method used for measuring viscosity was validated by measuring the viscosity of different base liquids (ultrapure water, water-ethylene glycol mixture, and pure ethylene glycol) in the temperature range of 20° C–50 °C. In order to measure viscosity with the highest possible accuracy in the calibration test, more than
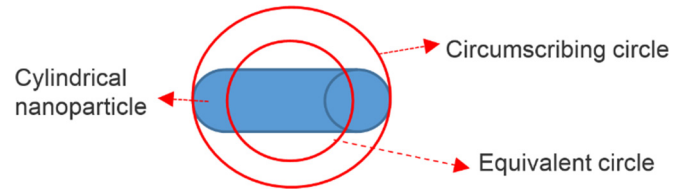

FIG. 2. Schematic drawing of the circumscribing and equivalent circles around a cylindrical nanoparticle.

200 sample points at different shear rates were selected. The average value of these measurements at each temperature was reported as the viscosity of the sample.

C. Identifying the relevant shape factor for thermal conductivity and viscosity

To quantify the particle shape, the shape parameter that is correlated to the thermophysical properties should be identified and evaluated. A recent study on sand investigated the correlation between several quantified shape parameters, such as elongation and sphericity, and geotechnical properties including thermal conductivity of sand specimens [56]. For nanofluids, however, it should be determined whether any of these shape parameters could be correlated to the relative thermal conductivity of the nanofluids. For example, the degree of resemblance of the particle to a sphere is known as sphericity but has different definitions in the literature [39,56,57]. In this study it is defined as the ratio of the diameter of the sphere that has the same surface area or volume as the particle (D_{eqs} or D_{eqv}) to the diameter of the circumscribing sphere of the nanoparticle (D_{cs}). The circumscribing and equivalent circles for a cylindrical particle are shown in Fig. 2. The particles presented in Table I can replace the cylinder shown in Fig. 2 and their corresponding sphericity can be calculated accordingly.

Elongation is another parameter, which measures how much a particle is elongated. It is defined as the maximum length to the minimum length in each particle. The ratio of the surface area to the volume of a particle is also considered as a shape parameter and its correlation to the thermal conductivity is investigated for silver nanofluid [58]. Since the surface area of the nanoparticle is in contact with the base fluid and conduction occurs by microscopic collisions of particles and movement of electrons within a body, we speculate that both the surface area and volume of the nanoparticle may play a vital role in the augmentation of the thermal conductivity.

Viscosity is defined as the measure of fluid's resistance to the deformation caused by the shear stress. As already mentioned, adding nanoparticles increases the viscosity of the nanofluid. Therefore, we focus on the behavior of the particle in the base fluid as the possible reason for the change in viscosity to find a correlation for the relative viscosity of the nanofluid. In general, dispersed particles could have two types of movement in the fluid: rotational motion and translational motion. As a result, the angular momentum and drag force are considered to evaluate this phenomenon. Angular momentum is defined as
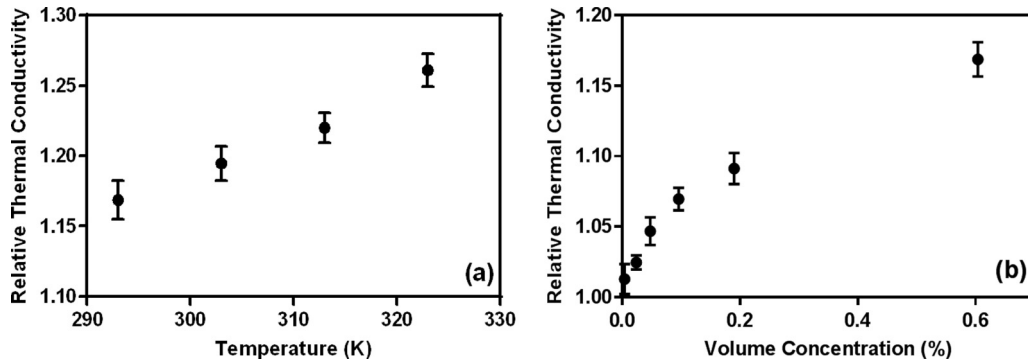
$$M = I\omega, \tag{7}$$

FIG. 3. Experimental measurement of relative thermal conductivity of spherical silver nanofluids versus (a) temperature at a volume concentration of 0.6 vol % and (b) volume concentration at a temperature of 293 K.

where M, I, and ω represent the angular momentum, mass moment of inertia, and angular velocity, respectively, and the mass moment of inertia of each particle is expressed as

$$I = \rho \int^{r^2} dV, \tag{8}$$

where ρ is the density, r is the perpendicular distance of the element, with a volume of dV, from the axis, and integration is over the entire body. In this study, the volume is constant for a nanoparticle with a different shape.

We assume that constant velocity is applied for all the particles and the drag force equation is defined as

$$F_D = \tfrac{1}{2}\rho v^2 C_D A, \tag{9}$$

where v is the speed of the particle relative to the base fluid, C_D is the drag coefficient, and A is the cross-sectional area of the particle normal to the direction of the motion. The density and speed of the particle are assumed to be constant in all cases and drag coefficient variation is negligible. Therefore, the cross-sectional area of the particle is the parameter that is considered to be correlated to the relative viscosity.

III. RESULTS AND DISCUSSION

A. Experimental study

Morphology and dynamic light scattering analyses of the silver-water nanofluid are performed. The scanning electron microscope and x-ray diffraction analyses were conducted for nanoparticles in a powder form. The thermal conductivity and viscosity of the silver nanofluids were experimentally investigated at various nanoparticle loadings and temperatures. Then the results of the present nanofluid were used to validate the correlation functions for relatively large particles.

Figures 3(a) and 3(b) show the relative thermal conductivity of silver nanofluids versus temperature and volume fractions, respectively. Relative thermal conductivity is defined as the ratio of the nanofluid thermal conductivity to the base-fluid thermal conductivity. For silver nanofluids, the range of volume fractions used was from 0 to 0.6% and temperature changed from 293 K to 323 K. For 0.6 vol %, the improvement in thermal conductivity is about 17% at 293 K and about 26% at 323 K. It is clear that the relative thermal conductivity increases almost linearly with the increase of

temperature. As stated by Das *et al.* [33], in nanofluids the most crucial item to increase the thermal conductivity is thought to be the stochastic motion of the nanoparticles. This Brownian-like motion is dependent on fluid temperature and so the enormous improvement in thermal conductivity with temperature is expectable. At low temperature, this Brownian-like motion is less critical in giving the characteristics of normal nanodispersion, which changes rapidly at elevated temperature, resulting in more nanoeffects in the conducting behavior of the fluid. It should be noted that this effect is debatable. For example, Gupta and Kumar found that the increase in thermal conductivity could be up to 6% [59]. Peñas *et al.* also observed different behavior of thermal conductivity versus temperature. For instance, as the temperature increases, the thermal conductivity enhancement of CuO nanofluids increases, while for SiO_2, the enhancement initially increases and then decreases [60]. In addition, the nanoparticle loading increased the thermal conductivity of the base fluid measured at 293 K. Different from the temperature, the effect of the nanoparticle concentration on the relative thermal conductivity is fairly nonlinear, ranging from 2% to 17%.

The relative viscosity, defined as the ratio of the viscosity of the nanofluid to the viscosity of the base fluid, of silver nanofluids under varying temperatures and volume fractions is also depicted in Figs. 4(a) and 4(b), respectively. Similar to the relative thermal conductivity, the relative viscosity of silver nanofluids increases linearly from 1.15 to 1.24 as the temperature increases from 293 K to 323 K. The data presented in Fig. 4(b) demonstrate that the viscosity was augmented slightly as the volume fraction was increased. This incremental behavior is apparently due to the increase of the overall surface area of the solid phase.

The increase of viscosity influences the transport process of nanofluid and necessitates higher pumping power. This is one of the drawbacks of using nanofluids. We must keep in mind that the main idea of using nanofluids in cooling applications is due to their higher thermal conductivity that requires less coolant liquid to circulate and thus lower pumping power.

B. Numerical study

In this section the results of EMD simulations considering the effect of shape, concentration, and temperature on thermal conductivity and viscosity of silver nanofluids will be
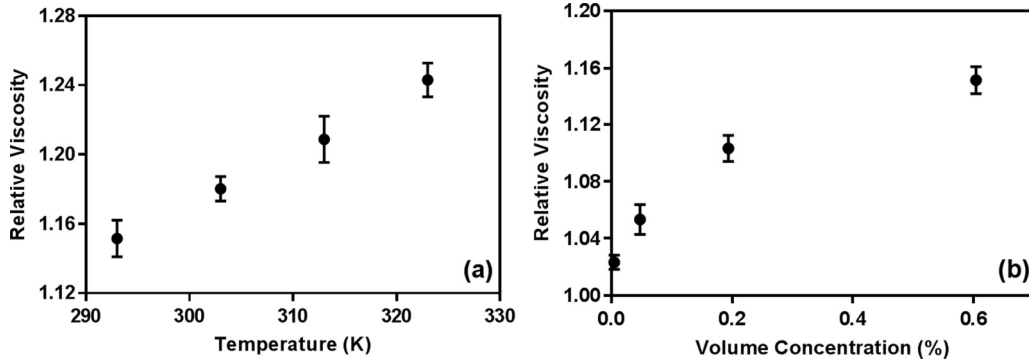
FIG. 4. Experimental measurement of relative viscosity of spherical silver nanofluids versus (a) temperature at a volume concentration of 0.6 vol % and (b) volume concentration at a temperature of 293 K.

discussed. As already discussed in Sec. II, elongation, sphericity, and surface area to volume ratio for thermal conductivity together with the moment of inertia and cross-sectional area for viscosity seem to be relevant shape parameters. Here we evaluate how they are correlated to the corresponding thermophysical property. It should be noted that the simulated system was relaxed at a temperature of 300 K. In addition, although the shape of the particles and the simulation box size vary in different MD simulations, the total volume concentration of the particles is kept constant (1 vol %) for all the cases in this section unless otherwise stated. The shape and dimensions of each particle are tabulated in Table I.

1. Effect of shape on thermal conductivity

Figure 5 shows the linear correlation between elongation, defined as the maximum to the minimum length of each particle, and relative thermal conductivity of the silver nanofluid. In general, it can be concluded that the relative thermal conductivity increases as the elongation increases. Based on this result, it seems that the conduction along a particle with a larger characteristic length is higher than a particle with the same volume but a smaller maximum length. However, it can be seen that the R^2 is quite low and data are not close to the fitted regression line. Hence, elongation is not
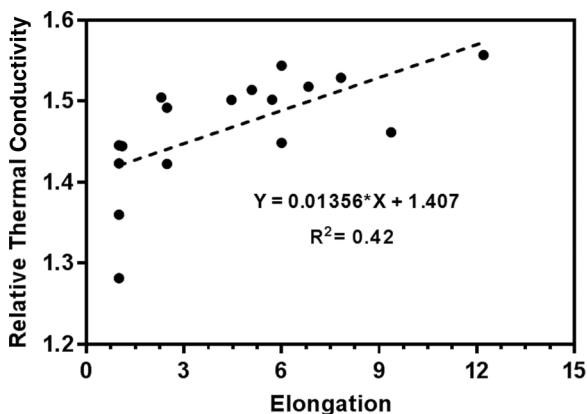
the suitable parameter to correlate particle shape with thermal conductivity.

Figure 6 presents the variation of the relative thermal conductivity with two different types of sphericity. Figure 6(a) shows the effect of the sphericity based on the surface area of the particle ($\frac{D_{eqs}}{D_{cs}}$) on the relative thermal conductivity, while Fig. 6(b) illustrates how the relative thermal conductivity changes with the volume-based definition of the sphericity ($\frac{D_{eqv}}{D_{cs}}$). It is expected that either sphericity has a value between 0 and 1.

In general, the relative thermal conductivity of a nanofluid is reduced as the shape of the particle becomes closer to a sphere. However, it could be seen that the value of the sphericity is always one for a sphere regardless of its size. Thus, sphericity alone cannot justify the thermal conductivity difference of the spherical nanoparticles with different sizes. In addition, for particles with a small sphericity value, such as long cylinders or long rectangular prisms, the relative thermal conductivity exhibits hysteric behavior. Moreover, the R^2 values from both fittings are low. Hence, it could be concluded that neither sphericity is an appropriate parameter to reveal the effect of particle shape on the thermal conductivity of a nanofluid.

Figure 7 shows the correlation between the surface area to volume ratio, namely, the aspect ratio (AR) and the relative thermal conductivity of the nanofluid. The graph clearly indicates that the thermal conductivity increases with an increase of AR. Among all the particles with a different shape but the same volume, the sphere has the lowest value of AR, while disks and pallets have greater values of AR. With the R^2 value of 0.94, the AR is the most correlated parameter, among all four shape factors investigated, to the thermal conductivity.

Having identified the appropriate shape factor for correlating the particle shape to the relative thermal conductivity of the nanofluid, we can further make it dimensionless. Considering the interaction between water and the silver nanoparticle, the finite distance at which the interparticle potential is zero (σ) can be used to make the aspect ratio dimensionless. Therefore, the dimensionless shape factor n for thermal conductivity is defined as

$$n = \sigma \frac{S}{V}, \tag{10}$$

where σ is constant and equals 3.0855 Å for our simulation.

FIG. 5. Relative thermal conductivity versus particle elongation of silver nanofluid at temperature 300 K and 1 vol %.
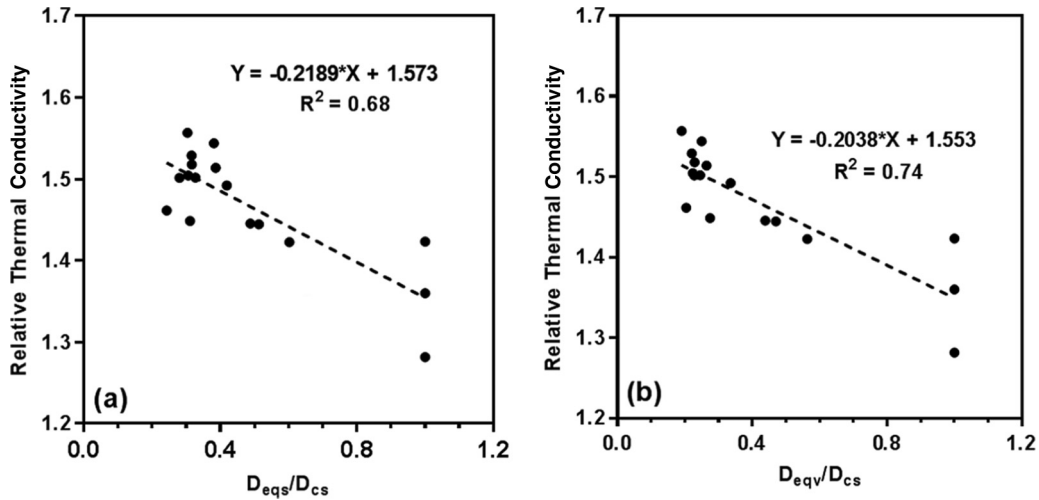
FIG. 6. Relative thermal conductivity versus (a) surface area-based sphericity and (b) volume-based sphericity of silver nanofluid at temperature 300 K and 1 vol %.

2. Effect of shape on viscosity

As mentioned previously, it is expected that two parameters, the cross-sectional area of the particle normal to the direction of the motion A and the geometrical term of the mass moment of inertia (B), may have an impact on the viscosity of the nanofluid. The different weighted average of these two parameters $(1 - \alpha)A + B\alpha$, namely, the viscosity shape factor (VSF), is investigated for the range of $0 \leqslant \alpha \leqslant 1$. Figure 8 shows the impact of the VSF on the viscosity of nanofluid in three directions based on α values of 0, 0.6, and 1. It could be observed that the viscosity is well correlated with the VSF with $\alpha = 0.6$ in all three directions. In particular, viscosity tends to increase linearly by increasing the VSF with $\alpha = 0.6$. However, when $\alpha = 0$, i.e., only the effect of the cross-sectional area is considered, or when $\alpha = 1$, i.e., only the effect of the mass moment of inertia is considered, the values of the viscosity in the three directions fluctuate considerably. It should be noted that other values of α, i.e., 0.1, 0.2, 0.4, 0.5, 0.7, and 0.9, have been investigated and among these values $\alpha = 0.6$ showed the strongest correlation
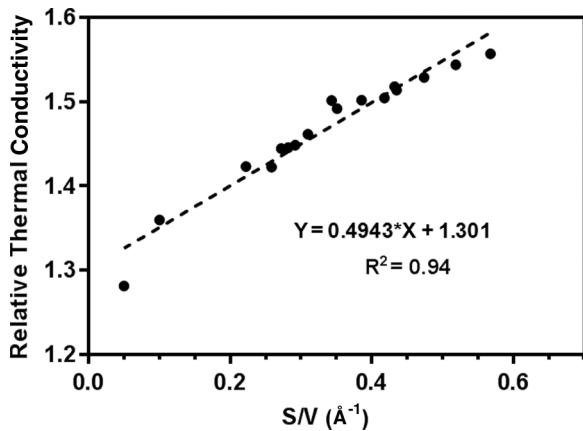

FIG. 7. Relative thermal conductivity versus surface area to volume ratio for different particle shapes of silver nanofluid at temperature 300 K and 1 vol %.

between the viscosity and the VSF. Therefore, the average values of the viscosity and VSF in the three directions with $\alpha = 0.6$ will be used in the next section as the shape factor to derive a correlation for the viscosity of nanofluid based on the shape of the nanoparticle. The unit for the VSF is length squared and in order to make it dimensionless, it is multiplied by σ^2,

$$m = \frac{\text{VSF}}{\sigma^2}, \tag{11}$$

by increasing the size of the nanoparticle, namely, increasing VSF; in other words, m increases.

3. Effect of concentration and temperature

In this section the effects of temperature and volume concentration on the thermophysical property of silver nanofluids are investigated. In the MD simulations in this section, a spherical nanoparticle with a diameter of 13.4 Å is used. The temperature varies from 280 K to 335 K, which is a range applied in many industrial sectors. In addition, the volume concentration is changed from 0.14% to 1.4%. In order to obtain the desired volume concentration, the size of the simulation box is changed accordingly as the spherical nanoparticle size is fixed.

Figure 9 presents the relationship between the simulated relative thermal conductivity and the temperature. Numerous studies on thermophysical investigations have shown that the thermal conductivity increases with increasing temperature. It is known that the primary reason for this phenomenon is the increase of the movement and vibration of atoms and molecules as temperature increases. For nanofluids, however, an additional mechanism, called microconvection, around the nanoparticle is speculated to increase the thermal conductivity. In this study, since the thermal conductivities of both the nanofluid and base fluid rise by increasing the temperature, the relative thermal conductivity increases with the temperature as well.

Figure 10 shows the effect of particle volume concentration on the relative thermal conductivity of silver nanofluid. It can
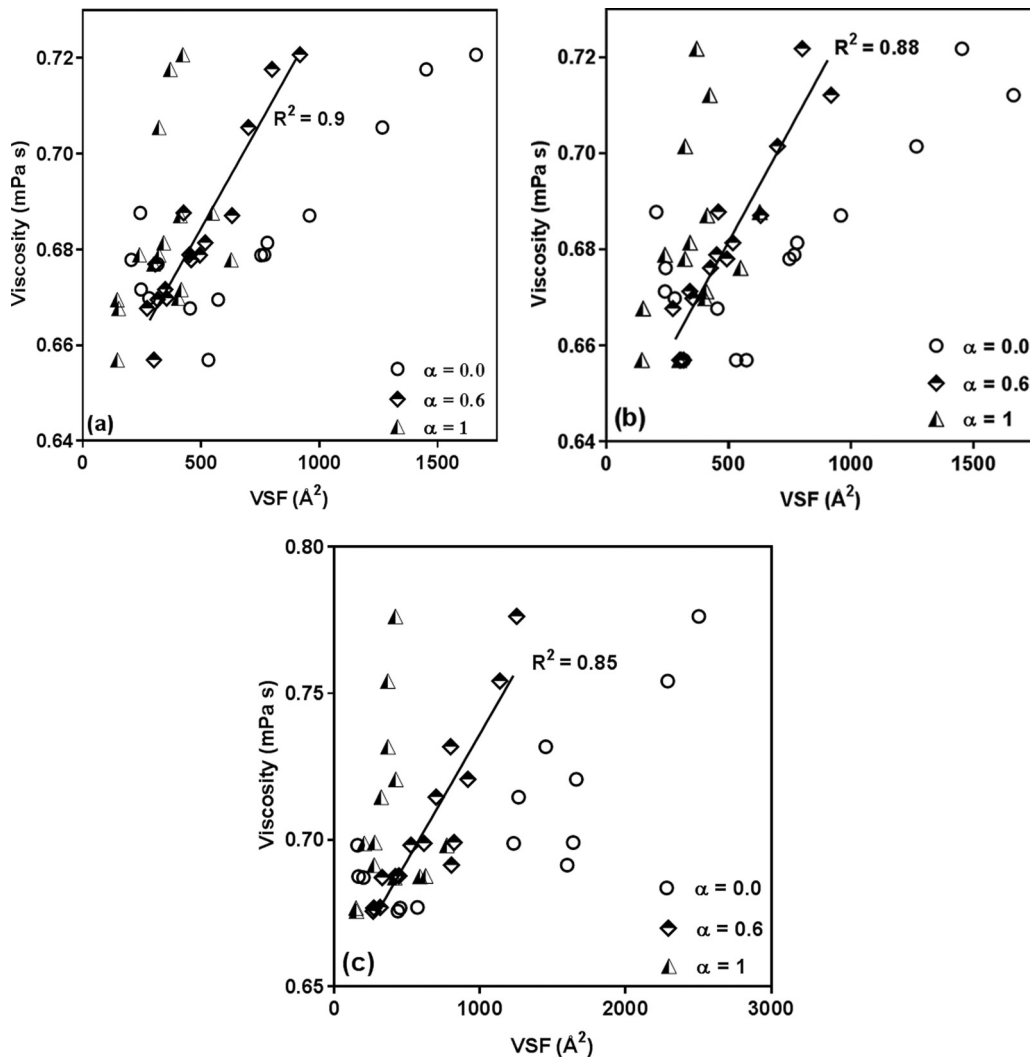
FIG. 8. Viscosity versus viscosity shape factor in the (a) x direction (b) y direction, and (c) z direction for three values of α.

be seen from Fig. 10 that the relative thermal conductivity increases constantly with the volume concentration. Loading a small number of silver particles into the water base fluid can

increase the thermal conductivity. For example, adding 0.14 vol % nanoparticles leads to an approximately 13% increase of the thermal conductivity and this augmentation could be
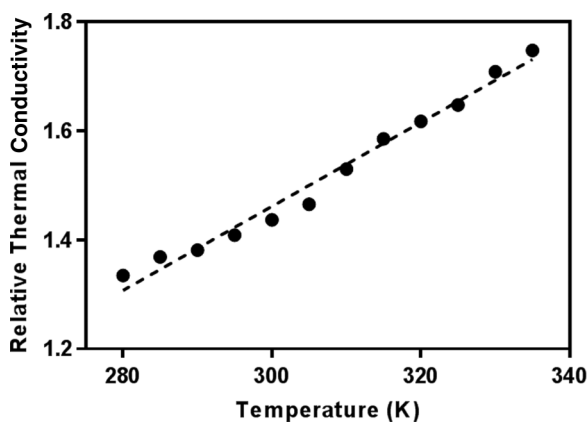
FIG. 9. Experimental measurement of the effect of temperature on the relative thermal conductivity of spherical silver nanofluid with 1.0 vol % concentration; the effect of temperature on volume concentration is neglected.
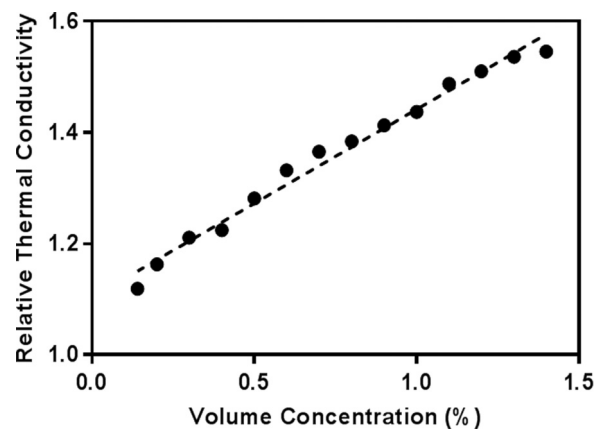

FIG. 10. Experimental measurement of the effect of the particle volume concentration on the relative thermal conductivity of spherical silver nanofluid at a temperature of 300 K; the effect of temperature on volume concentration is neglected.
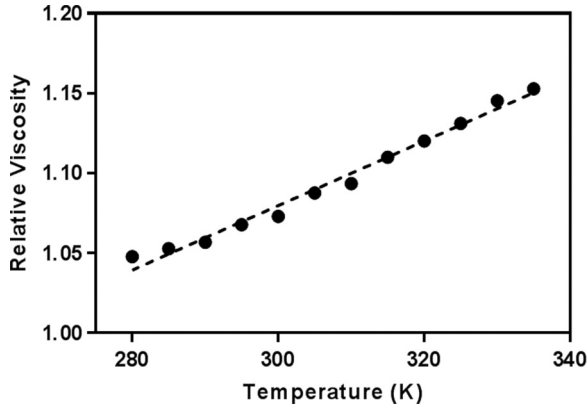
FIG. 11. Experimental measurement of the effect of temperature on the relative viscosity of spherical silver nanofluid at 1 vol %; the effect of temperature on volume concentration is neglected.

increased up to 53% under the highest concentration of 1.4 vol %.

Figure 11 shows how the relative viscosity increases when temperature rises in silver nanofluid with a 1% volume concentration. At lower temperatures, attractive intermolecular forces tightly bind the molecules together. The increase in temperature increases the kinetic or thermal energy. As a result, molecules become more mobile and can move more easily. Consequently, the viscosity of the liquid decreases. It is interesting to note that although the viscosity of the nanofluid decreases by increasing the temperature, the relative viscosity as the indicator of the difference between the viscosity values of the nanofluid and base fluid increases constantly with temperature. In other words, the temperature-dependent curves for the viscosity of the nanofluid and base fluid diverge as the temperature increases.

Figure 12 provides a change in the relative viscosity of the nanofluid by increasing the volume concentration of particles from 0.14% to 1.4%. It can be observed that the relative viscosity increases by increasing the particle loading linearly. Although, the volume loading of nanoparticles is known as one of the common methods for improving the thermal conductivity and heat transfer performance of nanofluids, the
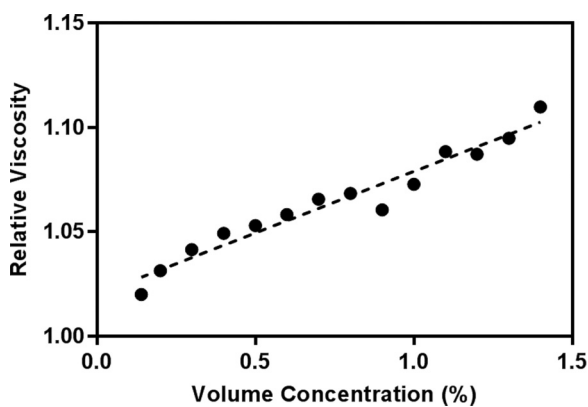

FIG. 12. Experimental measurement of the effect of particle volume concentration on the relative viscosity of spherical silver nanofluid at 300 K.

simultaneous increase of the viscosity, on the other hand, can have a negative impact in many applications. Therefore, it is always a trade-off between the thermal conductivity increase and the increased cost for pumping more viscous fluid. In particular, for silver nanofluid, the limit of volume concentration is observed to be around 1.4 vol %. Above this limit, the fluid will turn into gel and it could not be categorized as nanofluid anymore.

C. Development of the combined particle-shape-, temperature-, and concentration-dependent correlations

So far, the relationships of the temperature, volume concentration, and shape factor with thermal conductivity and viscosity of the silver nanofluid have been revealed by our EMD simulation. These simulation results are used to build correlations that combine all the selected physical variables in one expression. In order to obtain these correlations, dimensional analysis is applied. In this section the approach of developing two correlations for predicting thermal conductivity and viscosity is described and the proposed correlations are introduced. In this study EMD simulations are conducted to perform a systematic study of the effect of the particle shape, temperature, and volume concentration on thermal conductivity and viscosity of the nanofluids using our data collection method with the advantage of obtaining more reliable thermophysical properties. Two correlations for the thermal conductivity and viscosity of silver nanofluid will be developed based on these EMD simulations. Once validated by the experiments conducted in this study, these two correlations will be used to predict the thermophysical properties of nanofluids for much larger particle shape, temperature, and volume concentration ranges, which have previously been reported in the literature.

1. Correlation for the relative thermal conductivity

It has been discussed that the thermal conductivity of the nanofluid depends on particle shape, temperature, and volume concentration. In order to develop a correlation and combine all the selected physical variables in one expression, dimensional analysis is applied. Therefore, the resulting relationship between the thermal conductivity of the nanofluid and the aforementioned variables could be represented in dimensional form as

$$k_{nf} = f\left(k_{bf}, T, \varphi, \frac{S}{V}, \sigma\right). \tag{12}$$

The corresponding dimensionless groups can be selected as

$$\pi_1 = k_{nf}/k_{bf}, \tag{13}$$

$$\pi_2 = T/T_0, \tag{14}$$

$$\pi_3 = \varphi, \tag{15}$$

$$\pi_4 = \frac{S}{V}\sigma = n, \tag{16}$$
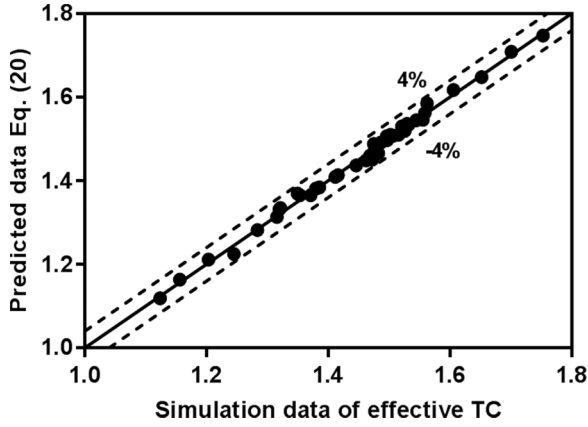
FIG. 13. Comparison of the MD simulation data with data predicted using Eq. (20).
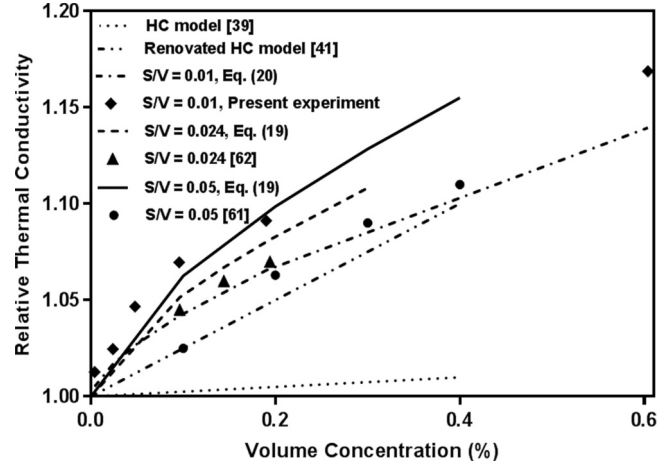

FIG. 14. Comparison of the relative TC data predicted by the proposed model and existing models with the data from the literature and the present experiment at different S/V (Å^{-1}) and volume concentrations at $T = 293$ K.

where the first dimensionless number evaluates the increase of thermal conductivity of the nanofluid (k_{nf}) related to that of the base fluid (k_{bf}). The reference temperature, i.e., $T_0 = 300$ K, is used to form the second dimensionless group (14). The nanofluid volume fraction is used to form the third dimensionless number as shown in Eq. (15). The dimensionless shape factor n is defined in Eq. (10). Then, one of the dimensionless groups can be considered as a function of the other groups as follows:

$$\pi_1 = f(\pi_2, \pi_3, \pi_4). \tag{17}$$

Based on experimental observations, $\frac{k_{nf}}{k_{bf}}$ (relative thermal conductivity) is a value normally greater than 1. Hence, the equation

$$\frac{k_{nf}}{k_{bf}} = 1 + E \tag{18}$$

can be derived, where E is defined as

$$E = a\left(\frac{T}{300}\right)^b (\varphi)^c (n)^d. \tag{19}$$

After a nonlinear regression of the simulation data represented in the preceding section along with a statistical analysis, the estimated values for the constants in Eq. (19) can be obtained and are expressed as

$$\frac{k_{nf}}{k_{bf}} = 1 + 9.89\left(\frac{T}{300}\right)^{4.75} (\varphi)^{0.65} (n)^{0.23}. \tag{20}$$

It should be noted that this equation is obtained for the following range of parameters:

$$0.14\% \leqslant \varphi \leqslant 1.4\%, \quad 280\,\text{K} \leqslant T \leqslant 335\,\text{K}. \tag{21}$$

Figure 13 compares the MD simulation results with the data predicted by Eq. (20). It should be noted that all data in Fig. 13 are the outcome of the EMD simulations. Initially, all simulation studies were conducted at 300 K with a volume concentration of 1% while the shape factors vary. At the next step, while the shape factor was fixed, namely, S/V is 0.22 Å ($n = 0.68$) and $m = 32$, the effect of temperature on particles with a volume concentration loading of 1% was investigated. Finally, the effect of a change in volume concentration on

thermal conductivity and viscosity by fixing shape factors was evaluated. All these data are depicted in Fig. 13 and are compared with the corresponding data predicted by Eq. (20). It can be found from Fig. 13 that the data obtained by Eq. (20) are very close to the MD simulation results. In fact, there is very good agreement between the predictions by the proposed correlation and the MD simulation data with a maximum standard deviation of 4%. Hence, it could be claimed that this model for thermal conductivity, Eq. (20), has been calibrated by the data from our MD simulations. In the next step, the proposed correlation will be validated by the data available from the literature as well as the data from our experimental results.

The experimental data points from the literature [61,62] with different volume concentrations and shape factors are compared with the predicted curves using Eq. (20) and representative existing models in Fig. 14. All data shown in this figure are obtained at 293 K. There is good agreement between the model predictions and the experimental data with a maximum standard deviation of 5%. This figure also shows that the conventional HC model [39] is not able to accurately predict the effect of the particle shape, while the recently developed HC correlation [41] shown by the dash–double-dotted line is in good agreement with the available results. The comparison suggests that the proposed TC model could be applicable to a wider range of S/V values in units of Å^{-1}.

A similar analysis is carried out to compare the relative thermal conductivity results of silver nanofluid with low and high particle volume concentrations at different temperatures. Figure 15 compares the results of our experiments (closed circles) with the predicted data (solid line) using Eq. (20). The figure shows that they are in good agreement and the maximum deviation is observed at 293 K, where the difference between the experimental and predicted results is 3.5%. It also shows that the relative thermal conductivity of the silver nanofluid at 0.04 vol % at different temperatures predicted by the proposed correlation is very close to the experimental data obtained by Parametthanuwat *et al.* [63]. A maximum
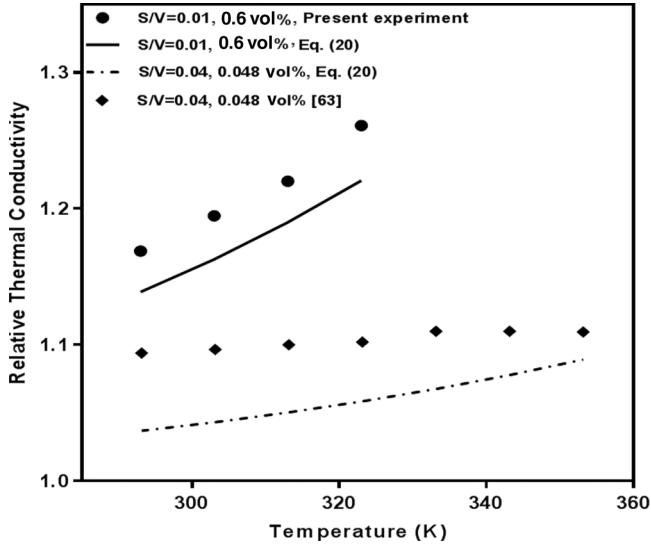
FIG. 15. Comparison of the relative TC data predicted by the proposed model with the measured data from the literature and the present experiment at different temperatures and volume concentrations.

deviation of 5% is observed at temperature 293 K. By increasing the temperature, the standard deviation decreases constantly until it reaches 1.8% at 353 K.

After confirming that Eq. (20) could be applied to particles with smaller values of S/V, it is interesting to investigate the effect of aspect ratios on the relative thermal conductivity of nanofluid. Figure 16 shows the behavior of the proposed correlation within the excessive range of shape factor S/V by comparing the results predicted by Eq. (20) with the MD simulation data. The results were obtained at $T = 300$ K and a particle volume of 1%. It could be seen that at low S/V, i.e., below 0.05, the relative thermal conductivity increases rapidly with S/V. However, after this point, an increase of the relative thermal conductivity gradually becomes slow and it eventually converges to a constant value. In other words, increasing S/V is very effective in enhancing the thermal conductivity in the low-S/V range. However, it becomes less effective as S/V increases further. It is known that S/V increases by
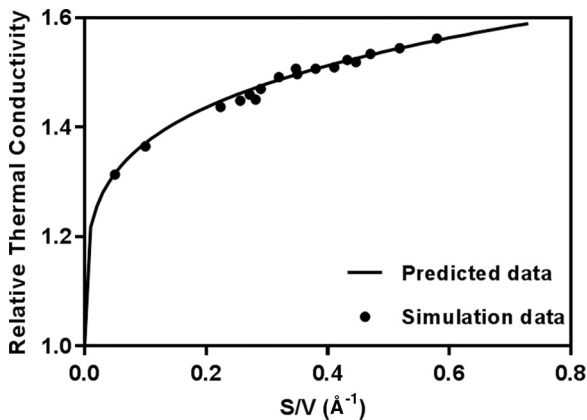

FIG. 16. Variation of the relative thermal conductivity with different S/V (Å^{-1}).

decreasing the size of the nanoparticle. It should also be considered that characterizing smaller particles requires more advanced technologies and consequently it is more expensive. Therefore, it is a trade-off between the costs of preparation and the benefits of replacing normal coolants with "expensive" nanofluids. Hence, in terms of the characterization and preparation of nanofluids, these aspects should be considered. In other words, the correlation introduced could be used as a guideline for selecting the shape and size of the silver nanoparticles before designing any experiments.

2. Development of the correlation for relative viscosity

A procedure similar to the relative thermal conductivity has been used to develop a correlation for the relative viscosity. A relationship between the viscosity of the silver nanofluid and physical variables could be represented as

$$\mu_{\mathrm{nf}} = f(\mu_{\mathrm{bf}}, \varphi, T, \mathrm{VSF}, \sigma). \tag{22}$$

Accordingly, the dimensionless groups

$$\pi_5 = \mu_{\mathrm{nf}}/\mu_{\mathrm{bf}}, \tag{23}$$

$$\pi_6 = T/T_0, \tag{24}$$

$$\pi_7 = \varphi, \tag{25}$$

$$\pi_8 = \frac{\mathrm{VSF}}{\sigma^2} = m \tag{26}$$

are selected, where the increase in viscosity of the nanofluid (μ_{nf}) related to that of the base fluid (μ_{bf}) is investigated by Eq. (23). The other dimensionless groups have already been described; in particular, the dimensionless shape factor m has been defined in Eq. (11). As a result, Eq. (22) can be rearranged and expressed in dimensionless form as

$$\pi_5 = f_1(\pi_6, \pi_7, \pi_8). \tag{27}$$

Similar to the relative thermal conductivity, the relative viscosity of the nanofluid normally has a value greater than one,

$$\frac{\mu_{\mathrm{nf}}}{\mu_{\mathrm{bf}}} = 1 + F, \tag{28}$$

where F is defined as

$$F = e\left(\frac{T}{300}\right)^f (\varphi)^g (m)^h. \tag{29}$$

By way of regression analysis, the MD simulation results related to temperature, volume concentration, and VSF are used and the following equation is obtained for the relative viscosity:

$$\frac{\mu_{\mathrm{nf}}}{\mu_{\mathrm{bf}}} = 1 + 2.83\left(\frac{T}{T_0}\right)^{5.2} (\varphi)^{0.88} m^{0.15}. \tag{30}$$

It should be noted that this equation is obtained for the following range of the parameters:

$$0.14\% \leqslant \varphi \leqslant 1.4\%, \quad 280\,\mathrm{K} \leqslant T \leqslant 335\,\mathrm{K}. \tag{31}$$

Figure 17 gives a comparison between the results obtained from our simulation and the results obtained using Eq. (30).
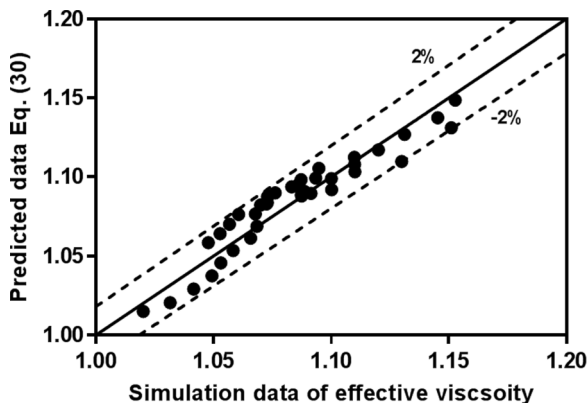
FIG. 17. Comparison of the simulation data with the data predicted by Eq. (30).

It could be seen that the standard deviation of the discrepancy is within 2%. Data points in Fig. 17 represent the outcome of the EMD simulations for the viscosity of silver nanofluid. Similar to simulations performed for thermal conductivity, these simulations for viscosity were conducted at 300 K, 1 vol %, $n = 0.68$, and $m = 32$. To study the effect of each factor (shape, temperature, or concentration), the corresponding factor is varied while the rest are kept constant.

Figure 18 compares the results predicted by Eq. (30) with the experimental data obtained at different m values and volume concentrations. All of the experiments from the present study and the literature [61,62] were conducted at a temperature of 293 K. There is only a less than 5% difference between the predicted and experimental results. The maximum difference is observed between the prediction and our experiment with an m value of 1.64×10^4. It should be noted that the maximum m that has been used in our numerical simulations is 657 and thus the parameters in Eq. (30) have not been calibrated by the data associated with m larger than 657. However, based on the comparison in Fig. 18, the proposed correlation could be extrapolated for particles with much
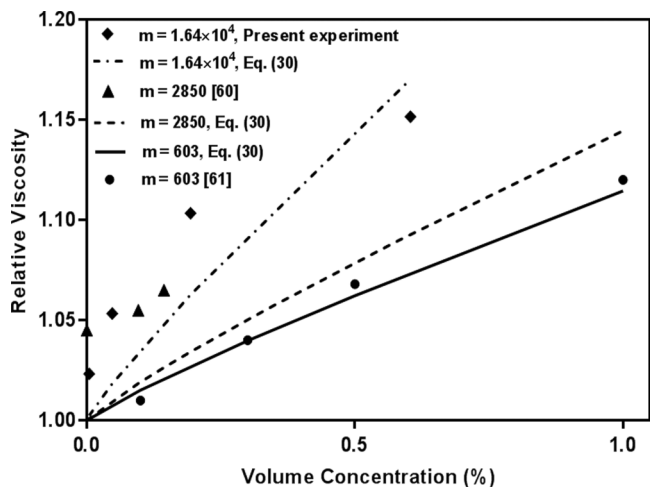

FIG. 18. Comparison of the relative viscosity data predicted by the proposed model with those in the literature and our experiment at different values of m and volume concentrations.
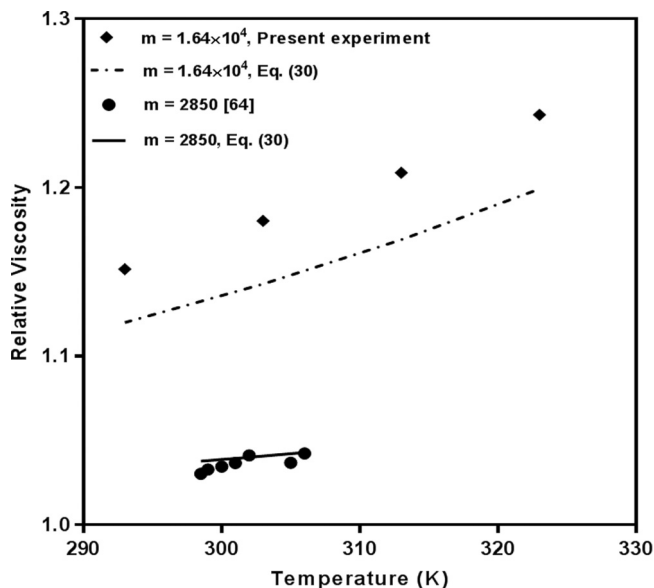

FIG. 19. Comparison of the relative viscosity data predicted by the proposed model with those in the literature and present experiment at different temperatures and volume concentrations.

larger m values. This figure also shows that for $m = 603$, the predicted relative viscosity values are in excellent agreement with the experiment data from [61].

Figure 19 shows the measured relative viscosity data from two experimental studies at different temperatures as well as their corresponding predictions obtained by Eq. (30). The present experiments used the particles with an m value of 1.64×10^4 and particle loading of 0.6 vol %, while Nakhjavani *et al.* [64] used particles with an m value of 2850 and particle loading of 0.1 vol %. The difference between the experimental and predicted results for the former is around 5%, while for the latter it decreases to 1.5%.

Figure 20 reports the effect of the m value on the relative viscosity at 300 K and 1 vol %. The solid line shows the predicted values from the correlation (30) and the closed circles are the MD simulation results. Based on this graph, the change in relative viscosity could be classified into two regions of m value: $0 < m \leqslant 35$ and $35 < m < \infty$. For the nanofluids with an m value of 35 or smaller, the change in
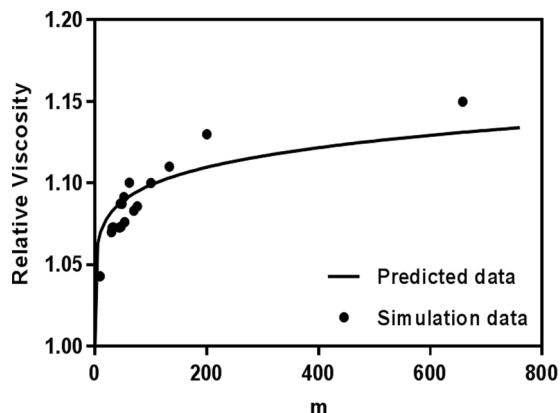

FIG. 20. Variation of relative viscosity at different values of m.

viscosity is highly dependent on the size and shape of the particle, and a smaller nanoparticle results in higher viscosity. However, as m increases to values greater than 35, the change of the viscosity is remarkably slower. It is interesting to note that the findings in the literature contradict each other on the effect of particle size on the relative viscosity as reported by Koca *et al.* [65]. Based on their review paper, while some studies show that the relative viscosity increases by decreasing the size of nanoparticles, others reported that the relative viscosity and particle size are in a direct positive relationship. Nevertheless, based on our study, it is found that an increase in the size of the particle reduces the relative viscosity.

IV. CONCLUSION

In this study thermophysical properties of water-based silver nanofluid have been investigated numerically and experimentally. Two correlations for the relative thermal conductivity and relative viscosity of nanofluids have been developed by considering the effect of temperature, concentration, and particle shape. The proposed correlations were validated by the available numerical simulation and experimental data.

It is worth noting that the data processing of EMD simulations relies on a recently developed method so that the accuracy of the numerical results is ensured. A comprehensive molecular dynamics simulation study was conducted to investigate the effect of different shape parameters on the thermal conductivity and viscosity of the nanofluid.

The effect of temperature and volume concentration on thermal conductivity and viscosity has been investigated. As expected, thermal conductivity increases when the temperature of the system rises. In contrast, the viscosity of the nanofluid decreases when its temperature increases. In regard to the relative viscosity and thermal conductivity, both increase when the temperature or volume concentration of the nanofluid rises.

This study has demonstrated that the shape of the nanoparticle is an important parameter. A wide range of particle shapes was investigated. Two parameters, defined as dimensionless numbers m and n, were introduced and their effect on the corresponding thermophysical properties was evaluated. It has been found that the surface to volume ratio is correlated to the thermal conductivity, while the mass moment of inertia

and the frontal cross-sectional area are correlated to the viscosity of the nanofluid.

Two correlations have been developed using the EMD simulation results as a function of temperature, volume concentration, and shape of the particle. Such a correlation has been developed for a wide range of particle shapes.

Although EMD simulations of this research show its ability to expand the horizon of the complexity of particle shape effect on thermophysical properties, this type of simulation has some constraints, such as a significant increase in the computation costs as the particle size increases. Therefore, our own experimental investigations together with the data available in the literature are used to expand the applicability range of the proposed correlation functions.

Results predicated by the proposed correlations have been compared with the data available in the literature and there is very good agreement between them. The maximum deviation is 5% in some cases and they clearly show that the proposed correlations are valid for a wide range of m and n values. It is worth comparing and combining the EMD simulation results of the present study with other data in the literature such that the proposed correlations are validated for and can be applied to nanofluids with larger particle shape, temperature, and volume concentration ranges than what have been simulated in this study.

Future studies on employing the proposed shape factors to a wider range of temperature could be performed. In particular, our study is restricted to the silver nanofluid, but a similar numerical study could be conducted for other nanoparticles to find a generalized form of the correlation, which will be valid for different nanofluids. Moreover, the effect of particle shape on the heat transfer coefficient and friction factor of the nanofluid flow is worth investigating using the proposed correlations.

[1] S. U. S. Choi and J. A. Eastman, Enhancing thermal conductivity of fluids with nanoparticles, *Conference: 1995 International Mechanical Engineering Congress and Exhibition* (ASME, San Francisco, CA, 1995).

[2] P. Samira, Z. H. Saeed, S. Motahare, and K. Mostafa, Korean J. Chem. Eng. **32**, 609 (2015).

[3] T. Hayat, S. Qayyum, M. Imtiaz, and A. Alsaedi, Int. J. Heat Mass Transfer **102**, 723 (2016).

[4] E. V. Timofeeva, A. N. Gavrilov, J. M. McCloskey, Y. V. Tolmachev, S. Sprunt, L. M. Lopatina, and J. V. Selinger, Phys. Rev. E **76**, 061203 (2007).

[5] S. Kondaraju, E. K. Jin, and J. S. Lee, Phys. Rev. E **81**, 016304 (2010).

[6] G. Karniadakis, A. Beskok, and N. Aluru, *Microflows and Nanoflows*, 1st ed. (Springer, New York, 2005), p. 123.

[7] I. Popa, G. Gillies, G. Papastavrou, and M. Borkovec, J. Phys. Chem. B **114**, 3170 (2010).

[8] M. Edalatpour and J. P. Solano, Int. J. Therm. Sci. **118**, 397 (2017).

[9] L. Zhang, Y. Jiang, Y. Ding, M. Povey, and D. York, J. Nanopart. Res. **9**, 479 (2007).

[10] M. Javanmardi and K. Jafarpur, J. Heat Transfer **135**, 042401 (2013).

[11] P. Sharma, I.-H. Baek, T. Cho, S. Park, and K. B. Lee, Powder Technol. **208**, 7 (2011).

[12] H. D. Koca, S. Doganay, and A. Turgut, Energ. Convers. Manage. **135**, 9 (2017).

[13] G. Paul, S. Sarkar, T. Pal, P. Das, and I. Manna, J. Colloid Interface Sci. **371**, 20 (2012).

[14] L. Godson, B. Raja, D. Mohan Lal, and S. Wongwises, J. Therm. Sci. Eng. Appl. **4**, 031001 (2012).

[15] M. Xing, J. Yu, and R. Wang, Int. J. Therm. Sci. **104**, 404 (2016).

[16] M. Behi and S. A. Mirmohammadi, Master's thesis, Royal Institute of Technology (KTH), Stockholm, Sweden, 2012, http://www.diva-portal.org/smash/get/diva2:561791/FULLTEXT02.pdf.

[17] D. Zhu, X. Li, N. Wang, X. Wang, J. Gao, and H. Li, Curr. Appl. Phys. **9**, 131 (2009).

[18] E. B. Haghighi *et al.*, Exp. Therm. Fluid Sci. **49**, 114 (2013).

[19] M.-S. Jeng, R. Yang, D. Song, and G. Chen, J. Heat Transfer **130**, 042410 (2008).

[20] C. Sun, W.-Q. Lu, J. Liu, and B. Bai, Int. J. Heat Mass Transfer **54**, 2560 (2011).

[21] M. M. Papari, F. Yousefi, J. Moghadasi, H. Karimi, and A. Campo, Int. J. Therm. Sci. **50**, 44 (2011).

[22] G. Puliti, S. Paolucci, and M. Sen, J. Nanopart. Res. **14**, 1 (2012).

[23] W. Cui, Z. Shen, J. Yang, and S. Wu, Appl. Therm. Eng. **76**, 261 (2015).

[24] W. A. M. Morgado and D. O. Soares-Pinto, Phys. Rev. E **79**, 051116 (2009).

[25] Y.-S. Lin, P.-Y. Hsiao, and C.-C. Chieng, Int. J. Therm. Sci. **62**, 56 (2012).

[26] P. L. Palla, C. Pierleoni, and G. Ciccotti, Phys. Rev. E **78**, 021204 (2008).

[27] M. S. Green, J. Chem. Phys. **22**, 398 (1954).

[28] R. Kubo, J. Phys. Soc. Jpn. **12**, 570 (1957).

[29] M. Caro, L. K. Béland, G. D. Samolyuk, R. E. Stoller, and A. Caro, J. Alloys Compd. **648**, 408 (2015).

[30] S. A. Mirmohammadi, L. Shen, and Y. Gan, Chem. Phys. Lett. **712**, 44 (2018).

[31] Q. Li, Y. Yu, Y. Liu, C. Liu, and L. Lin, Materials **10**, 38 (2017).

[32] M. Corcione, Energ. Convers. Manage. **52**, 789 (2011).

[33] S. K. Das, N. Putra, P. Thiesen, and W. Roetzel, J. Heat Transfer **125**, 567 (2003).

[34] C. Nguyen, F. Desgranges, G. Roy, N. Galanis, T. Maré, S. Boucher, and H. A. Mintsa, Int. J. Heat Fluid Flow **28**, 1492 (2007).

[35] J. A. Eastman, S. Choi, S. Li, W. Yu, and L. Thompson, Appl. Phys. Lett. **78**, 718 (2001).

[36] L. Chen, H. Xie, Y. Li, and W. Yu, Thermochim. Acta **477**, 21 (2008).

[37] E. V. Timofeeva, J. L. Routbort, and D. Singh, J. Appl. Phys. **106**, 014304 (2009).

[38] L. Yang, J. Xu, K. Du, and X. Zhang, Powder Technol. **317**, 348 (2017).

[39] R. L. Hamilton and O. Crosser, Ind. Eng. Chem. Fundam. **1**, 187 (1962).

[40] L. Yang, X. Xu, W. Jiang, and K. Du, Appl. Therm. Eng. **114**, 287 (2017).

[41] L. Yang and X. Xu, Int. Commun. Heat Mass Transfer **81**, 42 (2017).

[42] S. Stackhouse and L. Stixrude, Rev. Mineral. Geochem. **71**, 253 (2010).

[43] R. Vogelsang, C. Hoheisel, and G. Ciccotti, J. Chem. Phys. **86**, 6371 (1987).

[44] P. K. Schelling, S. R. Phillpot, and P. Keblinski, Phys. Rev. B **65**, 144306 (2002).

[45] H. Babaei, P. Keblinski, and J. M. Khodadadi, J. Appl. Phys. **112**, 054310 (2012).

[46] S. Sarkar and R. P. Selvam, J. Appl. Phys. **102**, 074302 (2007).

[47] W. G. Hoover, D. J. Evans, R. B. Hickman, A. J. Ladd, W. T. Ashurst, and B. Moran, Phys. Rev. A **22**, 1690 (1980).

[48] S. T. Cui, P. T. Cummings, and H. D. Cochran, Mol. Phys. **93**, 117 (1998).

[49] J. E. Jones, Proc. R. Soc. London Ser. A **106**, 463 (1924).

[50] M. S. Daw and M. I. Baskes, Phys. Rev. B **29**, 6443 (1984).

[51] L. A. Girifalco and V. G. Weizer, Phys. Rev. **114**, 687 (1959).

[52] P. Zarzycki, S. Kerisit, and K. M. Rosso, J. Phys. Chem. C **114**, 8905 (2010).

[53] S. Plimpton, J. Comput. Phys. **117**, 1 (1995).

[54] R. W. Hockney and J. W. Eastwood, *Computer Simulation Using Particles* (CRC, Boca Raton, 1988).

[55] W. G. Hoover, Phys. Rev. A **31**, 1695 (1985).

[56] C. Lee, H. S. Suh, B. Yoon, and T. S. Yun, Acta Geotech. **12**, 615 (2017).

[57] P. Barrett, Sedimentology **27**, 291 (1980).

[58] W. Cui, Z. Shen, J. Yang, S. Wu, and M. Bai, RSC Adv. **4**, 55580 (2014).

[59] A. Gupta and R. Kumar, Appl. Phys. Lett. **91**, 223102 (2007).

[60] J. R. V. Peñas, J. M. Ortiz de Zarate, and M. Khayet, J. Appl. Phys. **104**, 044314 (2008).

[61] H. U. Kang, S. H. Kim, and J. M. Oh, Exp. Heat Transfer **19**, 181 (2006).

[62] N. Nikkam and M. S. Toprak, Int. Commun. Heat Mass Transfer **91**, 196 (2018).

[63] T. Parametthanuwat, N. Bhuwakietkumjohn, S. Rittidech, and Y. Ding, Int. J. Heat Fluid Flow **56**, 80 (2015).

[64] M. Nakhjavani, V. Nikkhah, M. M. Sarafraz, S. Shoja, and M. Sarafraz, Heat Mass Transfer **53**, 3201 (2017).

[65] H. D. Koca, S. Doganay, A. Turgut, I. H. Tavman, R. Saidur, and I. M. Mahbubul, Renew. Sust. Energ. Rev. **82**, 1664 (2018).